

ASSESSMENT OF HIGH-PERFORMANCE COMPACT MICRO BARE-TUBE HEAT EXCHANGERS FOR ELECTRONIC EQUIPMENT COOLING

N. Kasagi¹, N. Shikazono¹, Y. Suzuki¹ & T. Oku²

¹ Department of Mechanical Engineering, The University of Tokyo, Hongo 7-3-1, Bunkyo-ku, Tokyo, 113-8656, Japan

² Nissan Motor Co., Ltd., Okatsukoku 560-2, Atsugi-shi, Kanagawa 243-0126, Japan

ABSTRACT

In the present study, a micro bare-tube heat exchanger without conventional fins is proposed and evaluated for electronic equipment cooling application. A micro bare-tube heat exchanger composed of 0.5mm outer diameter copper tubes is manufactured and tested experimentally. The optimal dimensionless transverse and longitudinal tube pitches were $P_T = 2.28$ and $P_L = 1.31$, respectively. It is shown that the resultant micro bare-tube heat exchanger can drastically reduce the core volume compared to the conventional plate fin and tube heat exchanger.

INTRODUCTION

Great efforts have been made for heat transfer augmentation, and a number of design concepts for compact heat exchangers have been proposed (e.g., see Kays and London [1]). Most of the gas-liquid heat exchangers adopt fins in order to compensate a lower heat transfer rate on the gas side. Paitoonsurikarn et al. [2] proposed a micro bare-tube heat exchanger, which was composed of a bundle of small diameter tubes without conventional fins. It was shown that the micro bare-tube heat exchanger had a possibility of improving heat exchanging performance and compactness with its high over-all heat transfer rate and large heat transfer area density.

Conventional liquid-air heat exchangers such that used for air conditioners and electronic equipment coolers generally require large heat transfer area and air flow rate because of the small thermal conductivity of air. This often increases the volume, noise and also initial and running costs of the total system. On the other hand, the micro bare-tube heat exchanger has a potential for improving air-side performance drastically, because both the heat conduction resistance of fins and the inner-tube heat resistance can be ignored compared to those of conventional heat exchangers. Moreover, it is possible to achieve a large heat transfer area density. This feature is really desirable for designing compact cooling systems. Paitoonsurikarn et al. [2] utilized the heat transfer and pressure drop correlations proposed by Zukauskas [3]. However, those correlations are not verified for predicting a wide range of tube arrangements and also at low Reynolds numbers, e.g., $Re < 500$, which is a characteristic Re range for compact heat exchangers.

In the present study, optimization method based on simulated annealing (SA) with a trained neural network representing the heat transfer and pressure drop

characteristics of a prescribed tube bank is introduced. A commercial CFD code, FLUENT5, was employed to train the neural network of this flow and thermal fields around various in-line tube bundle arrangements at low Reynolds numbers. Then an optimal micro bare-tube heat exchanger composed of 0.5 (mm) outer diameter copper tubes was manufactured and tested experimentally. The optimal dimensionless transverse and longitudinal tube pitches were $P_T = 2.28$ and $P_L = 1.31$, respectively. The experimental data were then directly utilized for the assessment of CPU cooling system. It is shown that the resultant micro bare-tube heat exchanger can drastically reduce the core volume compared to the conventional heat exchangers.

NUMERICAL SIMULATION OF FLOW AROUND IN-LINE TUBE BUNDLES

A commercial CFD code, FLUENT5, is employed to calculate the flow and thermal field around in-line tube bundles with three rows in the transverse direction and 10 columns in the longitudinal direction as shown in Fig. 1. The tube surface is assumed to be isothermal. Periodic boundary condition is employed in the transverse direction, and uniform velocity and free outflow conditions are given at inlet and outlet boundaries, respectively. The temperature dependence of the physical properties of working fluids is neglected.

The Reynolds number based on the tube diameter and the maximum velocity at the minimum cross section, Re_{max} , is varied in the range of $Re_{max}=10$ to 300. The dimensionless transverse and longitudinal tube pitches, P_T and P_L , are varied from 1.25 to 4.5. In total, 46 cases are calculated. It is known that three dimensionality of the flow is observed in the case of a single cylinder around $Re_{max}=100$. In the present study, however, two-dimensional unsteady calculation is performed because it is considered that the effect of three dimensionality of the flow on the mean heat transfer and pressure drop is negligibly small.

Finally, the Nusselt number Nu_i and the pressure coefficient C_p at i -th column are obtained by time

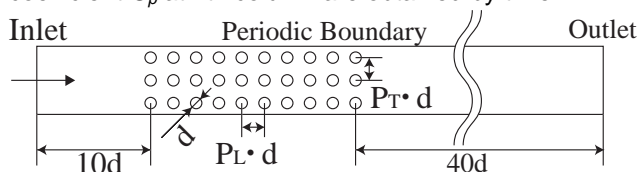


Fig. 1. Computational Domain.

averaging over several vortex shedding periods of a single cylinder at the same condition.

NEURAL NETWORK DATABASE

In order to obtain the optimal design of micro bare-tube heat exchangers, it is needed to interpolate accurately both heat transfer rate and pressure drop for wide ranges of tube pitches P_T , P_L and also of Re_{max} . Since it is not easy to correlate the CFD results with a simple algebraic expression, a neural network is employed to construct the heat transfer and pressure drop database from the CFD results.

Figure 2 shows the neural network structure proposed in this study. It is composed of three sub networks, NN1, NN2 and NN3. Input data are the tube pitches P_T , P_L and the Reynolds number Re_{max} , which is based on the tube diameter and the maximum bulk mean velocity at the narrowest cross section in between two tubes. The final output data are the Nusselt number and the pressure coefficient C_p . Sub neural network NN1 first outputs the Nusselt number and the drag coefficient of the first column, Nu_1 and $C_{D,1}$, and then these values are used as the input data for the second sub neural network of NN2. Sub neural network NN2 outputs Nu and C_D of the second column, and again those data are utilized as the input data for calculating the next downstream column. This iteration is repeated until NN2 reaches the final column, and finally sub network NN3 calculates the averaged Nusselt number Nu_{mean} and the sum of drag coefficients $C_p = \sum C_{D,i}$.

In the present study, a three layer neural network with the sigmoid activation function is employed. The number of neurons in the hidden layer is 3, 4 and 2 for NN1, NN2, and NN3, respectively. Synaptic weights are optimized using the backward propagation algorithm with a steepest gradient method. All 46 data points for various pitches and Reynolds numbers are used as a training data set.

The flow inside the tube is found to be in the laminar Re range for all the cases considered in this study. Thus, the heat transfer rate inside the tube is given by the analytical solution of Nusselt number under the isothermal condition:

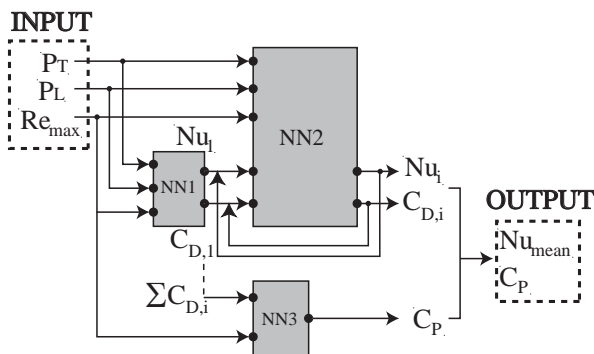


Fig. 2. Diagram of the Neural Network.

$$Nu_{in} = \frac{h_{in} d_{in}}{k_{in}} = 3.66. \quad (1)$$

The pressure drop of flow inside the tube is calculated by the following formula given by Kays and London [1]:

$$\Delta p_{core} = \frac{\rho U_m^2}{2} \left(K_c + K_e + f \frac{l}{d_{in}} \right), \quad (2)$$

where $f=64/Re_{in}$ is the friction factor, and K_c and K_e are the entrance and exit pressure loss coefficients, respectively. Those values for K_c and K_e are found in Kays and London [1]. The total pressure drop including the pressure drop at inlet and outlet manifolds is empirically assumed to be three times the core pressure drop, i.e.,

$$\Delta p_{in} = 3\Delta p_{core}. \quad (3)$$

OPTIMAL DESIGN BY SIMULATED ANNEALING

In this section, micro bare-tube heat exchanger is evaluated analytically by simulated annealing method. Generally, twelve design parameters must be optimized for micro bare-tube heat exchangers, as shown in Fig. 3. Some of these parameters are prescribed as design conditions and the rest are optimized so as to maximize or minimize the cost function.

One of the promising applications of micro bare-tube heat exchangers is the cooling system for electronic equipment. Semiconductor technologies have shown remarkable improvements over the decades, and the outlook of CPU power trend shows further increase. As a result, the cooling of those electronic devices is becoming crucial even for open server client systems. Figure 4 shows the schematic view of such cooling system. Heat is removed from the CPU by the cooling plate and transferred to the micro bare-tube heat exchanger by a single phase liquid. An aluminum block with a number of rectangular ducts is employed as a cooling plate in this study. The cost function employed for this case is the sum of the pumping power of coolant and the fan input for the micro bare-tube heat exchanger. In other words, total pumping power is minimized, while total heat exchange rate and volume are fixed.

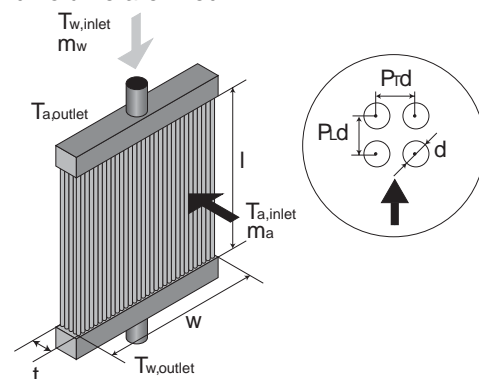


Fig. 3. Design Parameters of Micro Bare-Tube Heat Exchangers.

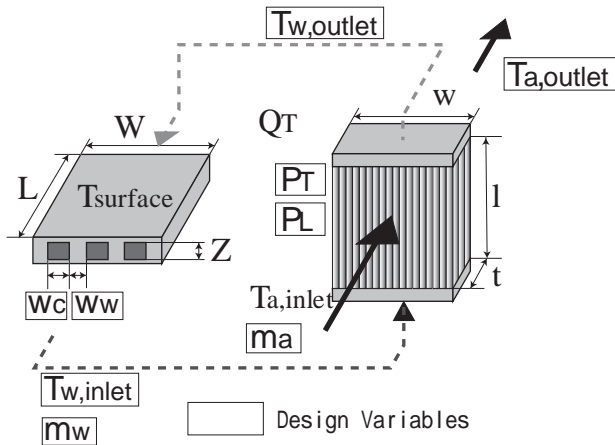


Fig. 4. Schematic View of Cooling System for Electronic Equipment.

With a set of governing equations, design parameters are optimized by using the simulated annealing method in such a way that they should minimize the cost function described above. The number of temperature steps and the number of random steps per a temperature step are both chosen as 1000. The temperature of the system is decreased according to a logarithmic annealing schedule with an arbitrary high starting temperature.

Figure 5 shows the total pumping power plotted against the heat exchange rate. The ratio of the heat exchanger core width, length and thickness are fixed as $w:l:t=5:5:1$. The value of a commercially available heat exchanger for a liquid cooling server is also plotted in the figure. It is shown that the micro bare-tube heat exchanger has a possibility of reducing drastically the core volume for the same pumping power and heat exchange rate.

Figure 6 shows the dimensionless transverse and longitudinal tube pitches of optimal micro bare-tube heat exchangers including other optimization examples such as automobile heat exchangers [4]. The specifications of tested heat exchangers are listed in Table 1. They are all typical commercial automobile heat exchangers. The cost functions employed for these heat exchangers are threefold, i.e., minimizing the pumping power, maximizing the heat exchanger rate, and minimizing the core volume. As can be seen from the figure, the optimal tube pitches gather around $P_T = 2.3$ and $P_L = 1.3$ for all cases. In these conditions, tubes are located closely in the flow direction while transverse tube pitch remains at a certain distance. It is thought that this

Table 1. Specifications of commercial heat exchangers.

| | Definition | Q (kW) | W (W) | w (m) | l (m) | t (m) | Vol (m ³) | T _{w,in} (°C) | T _{a,in} (°C) | m _a (kg/s) | m _w (kg/s) | Dp _a (Pa) | Dp _w (kPa) | W _a (W) | W _w (W) |
|----|-------------|--------|-------|-------|-------|-------|-----------------------|------------------------|------------------------|-----------------------|-----------------------|----------------------|-----------------------|--------------------|--------------------|
| H1 | Heater Core | 7.0 | 35.0 | 0.20 | 0.15 | 0.035 | 0.001050 | 80.0 | 15.0 | 0.116 | 0.2 | 343 | 2.93 | 34.3 | 0.59 |
| H2 | Heater Core | 6.4 | 21.0 | 0.20 | 0.15 | 0.025 | 0.000750 | 80.0 | 15.0 | 0.116 | 0.2 | 196 | 7.33 | 19.6 | 1.47 |
| R1 | Radiator | 59.3 | 277.4 | 0.65 | 0.43 | 0.016 | 0.004472 | 80.0 | 20.0 | 1.624 | 2.0 | 147 | 36.0 | 206 | 72.0 |
| R2 | Radiator | 76.8 | 456.2 | 0.65 | 0.43 | 0.027 | 0.007547 | 80.0 | 20.0 | 1.624 | 2.0 | 294 | 22.7 | 412 | 45.3 |
| R3 | Radiator | 146.5 | 782.4 | 0.70 | 0.75 | 0.050 | 0.026250 | 80.0 | 20.0 | 3.050 | 2.0 | 294 | 4.93 | 811 | 10.1 |

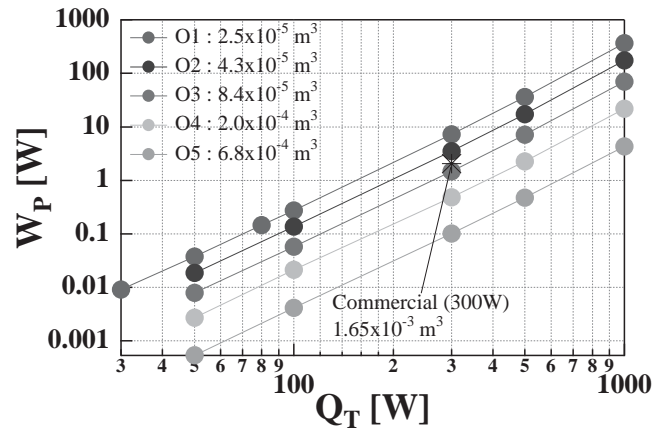


Fig. 5. Total Pumping Power Against Heat Exchange Rate at Various Core Volumes for Optimization Case 4.

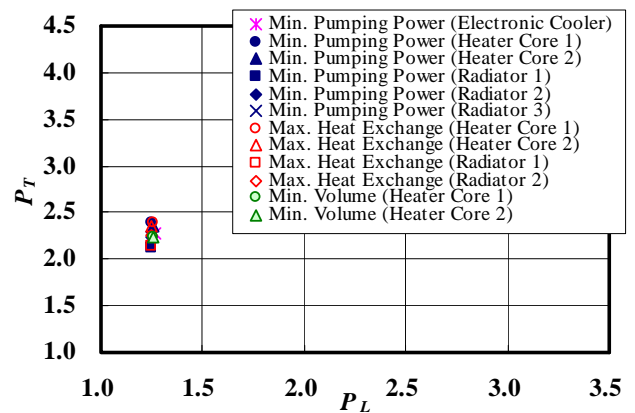


Fig. 6. Dimensionless optimal transverse and longitudinal tube pitches for all cases.

tube arrangement can maximize the heat transfer area while the increase of maximum air velocity between the tubes is suppressed. As a result, the air flow through this tube arrangement resembles to that through parallel plates. These optimal tube pitches were found to be independent of tube diameter whose optimal values varied from $d_o = 0.14$ to 0.74 (mm) for the cases plotted in Fig. 6.

From simulated annealing simulations, advantages of micro bare-tube heat exchanger can be recognized. In the following sections, micro bare-tube heat exchanger is manufactured and tested in order to confirm its performance experimentally.

EXPERIMENTAL APPARATUS AND PROCEDURE

Micro bare-tube heat exchanger composed of 0.5 (mm) outer diameter copper tubes was manufactured. The core height, width and thickness of the heat exchanger are, 50 mm, 50 mm and 10 mm, respectively. The dimensionless transverse and longitudinal tube pitches were set as $P_T = 2.28$ and $P_L = 1.31$ from the

simulated annealing result. The total number of tubes thus becomes 645 (43 × 15).

The experimental apparatus is shown in Fig. 7. The air flows through the filter and the wire mesh to obtain homogeneous inlet velocity field and then enters to the test section and to the heat exchanger. The air flow rate was measured by a gas flow meter (Yamatake Ltd. CMG250), and pressure drop was measured by a dipping bell manometer. Hot water (60 °C) was supplied by the circulator and the pump, where the water flow rate was measured by a float type flow meter. As water side heat exchange rate includes heat loss from the manifold and the duct, air side heat exchange rate was utilized for calculating heat transfer coefficient. The uncertainty of the measured air side heat exchange rate was estimated to be within ± 7%.

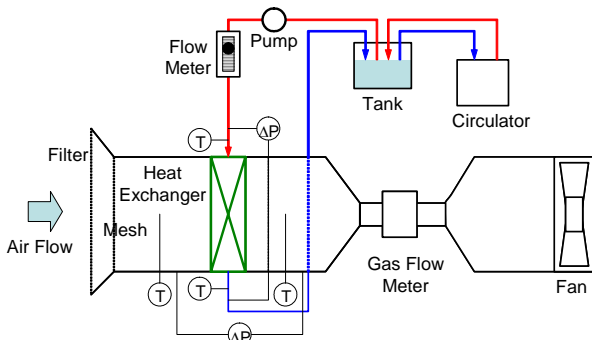


Fig. 7. Experimental Apparatus.

The air side heat transfer coefficient was calculated by ε -NTU method for cross flow configuration:

$$\varepsilon = 1 - \exp \left[\left(\frac{1}{C_r} \right) NTU^{0.22} \left\{ \exp \left[-C_r NTU^{0.78} \right] - 1 \right\} \right], \quad (4)$$

$$\varepsilon = \frac{Q_{measured}}{C_a (T_{w,inlet} - T_{a,inlet})}, \quad (5)$$

$$C_r = C_w / C_a, \quad (6)$$

$$NTU = \frac{KA}{C_a}, \quad (7)$$

$$\frac{1}{K} = \frac{d_{out}}{d_{in}} \frac{1}{h_{in}} + \frac{1}{h_{out}} + \frac{d_{out}}{2k} \ln \left(\frac{d_{out}}{d_{in}} \right), \quad (8)$$

where ε and NTU are temperature effectiveness and number of transfer unit, C_a and C_w are the heat capacity of the air and water flows, respectively. Since all experiments were carried out for the laminar Re range for water side, in-tube heat transfer coefficient h_{in} was calculated using Eq. (1).

EXPERIMENTAL RESULTS

The pressure loss of the air side ΔP_a is plotted against frontal air velocity in Fig. 8. The solid line denotes the predicted curve obtained from neural network. Present experimental results show good agreement with the neural network prediction.

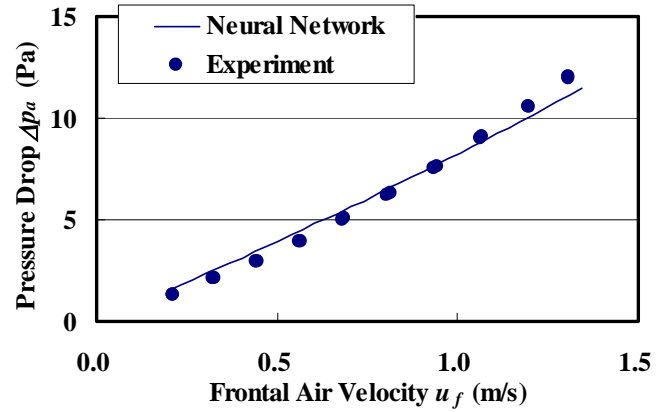


Fig. 8. Air side pressure drop.

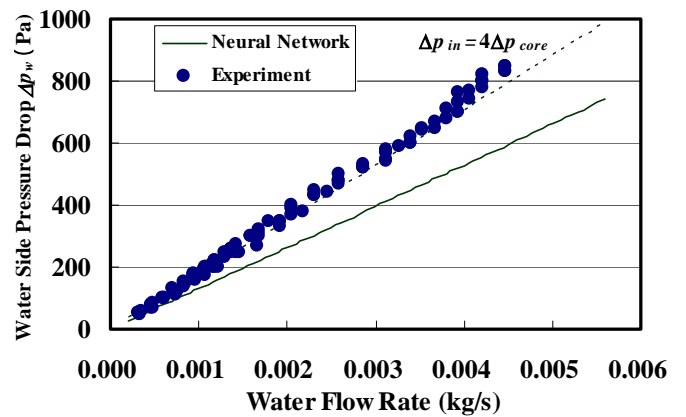


Fig. 9. Water side pressure drop.

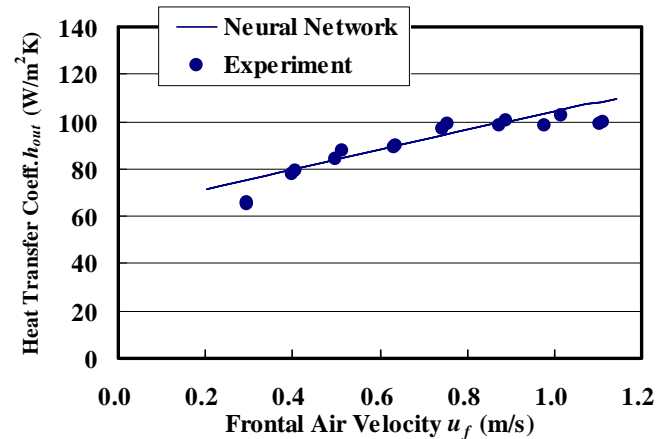


Fig. 10. Air side heat transfer coefficient

Water side pressure drop data ΔP_w are compared with the neural network result in Fig. 9. From Eq. (3), the neural network prediction assumes empirical relation for the effect of pressure loss at inlet and outlet manifolds, i.e., $\Delta p_{in} = 3\Delta p_{core}$. The present experiment implies that this additive pressure loss must be larger than expected, and should be treated with a larger multiplier value. In Fig. 9, $\Delta p_{in} = 4\Delta p_{core}$ curve is plotted as a dashed line, which seems to agree better with the

present result.

Since in-tube flow conditions are always laminar for the present experiment conditions, water side heat transfer coefficients are calculated from Eq. (1). Then, the air side heat transfer coefficient can be derived from Eqs. (4) to (8). The obtained experimental result shown in Fig. 10 is in good agreement with the neural network prediction. It must be noted that in case of micro bare-tube heat exchangers, the in-tube heat resistance and tube wall conductance can be ignored. Thus, air side heat transfer coefficient gives nearly the same value as the overall heat transfer coefficient. It is emphasized that the obtained experimental value for the overall heat transfer coefficient is very high and satisfactory.

ASSESSMENT OF MICRO BARE-TUBE HEAT EXCHANGER FOR CPU COOLING APPLICATION

In this section, micro bare-tube heat exchanger is evaluated using the experimental results. Main target is high-end sever CPU cooling system. Since the CPU power trend shows further increase, the cooling of those electronic devices is becoming crucial especially for high-end servers. Design constraints are the CPU heat dissipation, and the heat exchanger frontal area. Design specifications for the conventional plate fin and tube heat exchanger of 7mm diameter tube are shown in Table 2. The empirical correlation proposed by Fujii and Seshimo [5] for plate fin and tube heat exchanger is used for estimating the heat transfer performance of conventional heat exchanger. Since the frontal area of the heat exchanger is restricted from the requirement of system compactness, the heat exchanger thickness in flow direction becomes very large.

Same configurations for the micro bare-tube heat exchanger as the one tested in the previous section, i.e., tube diameter and pitches, are adopted here. We also assume that the effect of thickness, i.e., number of columns in flow direction, on the heat transfer and pressure drop can be neglected. These assumptions allow us to utilize previous experimental results directly for investigating the feasibility of micro bare-tube heat exchanger for CPU cooling. Both experimental data for air side heat transfer coefficient and pressure drop are expressed as a function of Reynolds number based on maximum velocity and tube outer diameter. The following correlations are derived and utilized hereafter for the assessment:

$$Nu_{out} = \frac{h_{out}d_{out}}{k_a} = 0.5919 \left(\frac{u_{max}d_{out}}{\nu_a} \right)^{0.2901}, \quad (9)$$

$$C_{Pout} = \frac{\Delta P_a}{N_L \left(\frac{1}{2} \rho u_{max}^2 \right)} = 6.9083 \left(\frac{u_{max}d_{out}}{\nu_a} \right)^{-0.7799}. \quad (10)$$

Air flow rate and heat exchanger thickness are optimized while total heat exchange rate and pumping power are fixed to the same values as the conventional plain fin and tube heat exchanger. The optimal result

for micro bare tube heat exchanger is also listed in Table 2. It can be seen that the core volume of the micro bare-tube heat exchanger is 89% smaller than that of the conventional plate fin and tube heat exchanger. The freedom of system design drastically increases if the core volume (thickness) of heat exchanger is reduced. For example, it is easy to bend those thin heat exchangers and to place it so that the substantial cross section area of the air flow becomes large. System performance can be improved if the frontal area of heat exchanger is enlarged, because the low air side pressure drop will lead to low pumping power and fan noise. Thus, it can be said that micro bare-tube heat exchanger is promising for CPU cooling application. However, the optimal number of columns is larger than the test sample. This effect must be investigated in the future research.

Comparing the optimal operating conditions for the two heat exchangers, large diversity is found on the values of temperature effectiveness ϵ . Temperature effectiveness of micro bare-tube heat exchanger is much lower than that of the conventional heat exchanger. In other words, micro bare-tube heat exchanger operates under larger air flow rate, while the pressure drop remains small compared to plate fin and tube heat exchanger. This is due to the fact that micro bare-tube heat exchanger can achieve considerably high overall heat transfer coefficient because in-tube and conduction

Table 2. Comparison of micro bare-tube heat exchanger and conventional plate fin and tube heat exchanger.

| | | Conventional Plate Fin and Tube | Micro Bare-Tube | | |
|---------------------|------------------------------|---------------------------------|-----------------|--------|-------|
| Specification | Tube Diameter | mm | 7.0 | 0.5 | |
| | Tube Pitch | Transverse | mm | 25.4 | 1.140 |
| | | Longitudinal | mm | 10.5 | 0.655 |
| | Number of Rows | | 3 | 57 | |
| | Number of Columns | | 12 | 21 | |
| | Fin Pitch | mm | 1.49 | - | |
| | Air Side Heat Transfer Area | mm ² | 0.379 | 0.0716 | |
| | Heat Exchanger Height | mm | 38.1 | 38.1 | |
| | Heat Exchanger Width | mm | 65.0 | 65.0 | |
| | Heat Exchanger Thickness | mm | 126.0 | 13.6 | |
| Core Volume | mm ³ | 312039.0 | 33680.4 | | |
| | | 100% | 11% | | |
| Operating Condition | Water Flow Rate | g/s | 6.546 | 6.546 | |
| | Air Flow Rate | m ³ /min | 0.30 | 0.412 | |
| | Water Inlet Temperature | | 65.0 | 65.0 | |
| | Water Outlet Temperature | | 59.5 | 59.5 | |
| | Air Inlet Temperature | | 35.0 | 35.0 | |
| | Air Outlet Temperature | | 54.6 | 54.5 | |
| | Frontal Velocity | m/s | 2.02 | 2.77 | |
| | Air Side Heat Transf. Coeff. | W/m ² K | 69.9 | 136.2 | |
| | Overall Heat Transf. Coeff. | W/m ² K | 40.0 | 132.4 | |
| | Temperature Effectiveness | - | 0.91 | 0.65 | |
| | Air Side Pressure Drop | Pa | 57.7 | 41.6 | |
| | Water Pumping Power | mW | 1.1 | 4.1 | |
| | Air Pumping Power | mW | 288.3 | 285.3 | |
| | Total Pumping Power | mW | 289.4 | 289.4 | |
| | Heat Exchange Rate | W | 150 | 150 | |

heat resistances are negligible. Micro bare-tube heat exchanger is promising especially for applications where frontal area of the heat exchanger is restricted and air side pressure drop is critical.

CONCLUSIONS

In the present study, the following conclusions are derived:

1. The Nusselt number and the pressure coefficient of micro bare-tube heat exchangers largely depend on the Reynolds number and the tube pitches, P_T and P_L . The data obtained by numerical simulation are correlated by a neural network composed of three sub-networks.
2. Micro bare tube heat exchanger is optimized by the simulated annealing method. The micro bare-tube heat exchangers show large improvement over conventional heat exchangers. The optimal transverse and longitudinal tube pitches for all cases are found to be around $P_T=2.28$ and $P_L=1.31$, respectively.
3. Micro bare-tube heat exchanger composed of 0.5 (mm) outer diameter copper tubes was manufactured and tested experimentally. Air side heat transfer coefficient and pressure drop were in good agreement with the neural network prediction, while water side pressure drop was nearly 35% larger than prediction. The effect of inlet and outlet manifolds on water side pressure drop seems to be large, and $\Delta p_{in}=4\Delta p_{core}$ is recommended from the present experiment.
4. Micro bare-tube heat exchanger was evaluated for the CPU cooling application. Experimental results were directly used for obtaining optimal design. It showed 89% reduction in core volume when total heat exchange rate and pumping power were fixed equal to that of the conventional plate fin and tube heat exchanger. It is concluded that micro bare-tube heat exchanger is very effective for applications where compactness is strongly required.

ACKNOWLEDGEMENT

This work was supported through the Grant in Aid for Scientific Research (A) (No.13305015) by the Ministry of Education, Culture, Sports, Science and Technology. The authors would also like to thank Ms. Mari Ono for her support through the experiment.

NOMENCLATURE

A Heat transfer area, m^2
 C Heat capacity of the flow, W/K
 C_D Drag coefficient, $\Delta p/(\rho u_{max}^2/2)$
 C_p Pressure coefficient, ΣC_D
 d Tube diameter, m
 f Friction factor, $64/Re_{in}$
 h Heat transfer coefficient, W/m^2K
 K Overall heat transfer coefficient, W/m^2K

k Thermal conductivity, W/mK
 l Heat exchanger height, m
 m Mass flow rate, kg/s
 N Number of tubes
 NTU Number of transfer unit
 Nu Nusselt number, hd/k
 p Pressure, Pa
 P_T Transverse pitch
 P_L Longitudinal pitch
 Q Heat exchange rate, W
 Re_{in} In-tube Reynolds number, $u_m d_{in}/\nu$
 Re_{max} Reynolds number, $u_{max} d/\nu$
 t Heat exchanger thickness, m
 T Temperature, K
 w Heat exchanger width, m
 W Pumping power, W
 ε Temperature effectiveness
 ρ Density, kg/m^3
 ν Kinematic viscosity, m^2/s
Subscripts
 a air
 i i-th column
 in inner
 m mean
 max maximum
 out outer
 w water

REFERENCES

1. W. M. Kays and A. L. London, *Compact Heat Exchangers 3rd edition*, John Wiley & Sons (1984).
2. S. Paitoonsrikarn, N. Kasagi and Y. Suzuki, Optimal Design of Micro Bare-Tube Heat Exchanger, Proc. Symp. Energy Eng. in the 21st Century, Vol. 3, pp. 972-979 (2000).
3. A. Zukauskas, Heat Transfer from Tubes in Cross Flow, Adv. in Heat Transfer, pp. 93-160 (1972).
4. N. Kasagi, Y. Suzuki, N. Shikazono & K. Oku, Optimal Design and Assessment of High Performance Micro Bare-Tube Heat Exchangers, To appear in 4th Int. Conf. Compact Heat Exchangers Enhancement Technology for the Process Industries (2003)
5. M. Fujii and Y. Seshimo, Heat Transfer and Friction Performance of Plate Fin and Tube Heat Exchangers at Low Reynolds Numbers (3rd Report, Generalized Correlation of Performance (in Japanese), Trans. Jpn. Soc. Mech. Engrs., Vol. 53, No.490, pp. 1767-1772 (1987)